J. Inst. Eng. India Ser. C (April 2021) 102(2):553–562
https://doi.org/10.1007/s40032-020-00655-7

ARTICLE OF PROFESSIONAL INTERESTS

Experimental Study on the Performance Enhancement of the Photovoltaic Cells by Using Various Nano-Enhanced PCMs

H. A. Refaey[1,2] · M. H. Wahba[1] · H. E. Abdelrahman[1] · M. Moawad[1] · N. S. Berbish[1]

Received: 8 July 2020 / Accepted: 27 December 2020 / Published online: 5 January 2021

Abstract The present paper presented an experimental work to enhance the photovoltaic cells performance. A heated aluminum plate is used to simulate the PV solar cell. The effect of different phase change material (PCM) type, heat sink configurations, PCM mixed with Al_2O_3 nanoparticles at different volumetric concentrations from 0.11 to 0.77% are experimentally investigated. The PCMs used are RT28HC, RT35HC and RT44HC which have melting point near the PV solar cell reference temperature. Three different heat sinks of hollow cylindrical fins, 11, 18 and 22 fins, are used to act as thermal conductivity enhancer (TCE) to improve the heat transfer rate to the PCM and achieve uniform heat distribution within the PCM. The experiments are carried out for free surface-simulated PV solar cell, simulated PV solar cell with heat sink only, simulated PV solar cell with heat sink and pure PCM and finally simulated PV solar cell with heat sink and PCM with nanoparticles. The results show good enhancement in the reduction in front surface temperature and the highest enhancement is 57.7% that occurs at heat flux of 820 W/m^2 and 22 hollow cylindrical copper fins immersed in the mixture of RT44HC-Al_2O_3 nanoparticles with concentration of 0.77% by volume at $T_\infty = 21 \pm 1$ °C.

✉ H. A. Refaey
hassanein.refaey@feng.bu.edu.eg

✉ M. H. Wahba
hosni_wahba@yahoo.com

[1] Department of Mechanical Engineering, Faculty of Engineering at Shoubra, Benha University, 11629 Cairo, Egypt

[2] Department of Mechanical Engineering, College of Engineering at Yanbu, Taibah University, Yanbu 41911, Saudi Arabia

Keywords PCM · Nanoparticles · Thermal conductivity enhancer · Photovoltaic cells · Heat sink · Heat storage capacity

Abbreviation

A	area, m^2
Conf.	Configuration
FST	Front surface temperature
H	Fin height, mm
N	Number of fins
PCM	Phase change material
Q	Heat flux, W/m^2
S	Spacing
T	Temperature, °C
t	Time, min
TCE	Thermal conductivity enhancer
TES	Thermal energy storage
U	Overall heat transfer coefficient, W/m^2.K

Subscript

E	Enclosed
R	Root
PV	Photovoltaic
L	Longitudinal
T	Transversal

Greek letters

∞	Ambient
$\tau\alpha$	Effective transmittance-absorptance of solar cell (optical efficiency)

Introduction

Nano-PCM with high heat storage capacity helps photovoltaic module to avoid the increase in temperature especially by fixing copper heat sinks at the rear surface of PV.

Saha et al. [13] presented experimental and numerical studies to investigate the effectiveness and performance of a TSU as a thermal management device for electronic components. For the configuration studied, the lowest operating temperatures are attained with about 8% volume fraction of TCE and with a larger number of fins. It is found that the duration of constancy of temperature is directly related to the amount of PCM, but the value of that constant temperature depends on the volume fraction of TCE. Saha and Dutta [14] studied numerically and experimentally thermal management of electronics using PCM-based heat sink subjected to cyclic heat load. A modified PCM-based heat sink was designed such that the thermal resistance of the heat flow path during the cooling period was significantly reduced and was comparable to that of heat flow path during the heating period. It was found that the performance of modified PCM-based heat sink was superior to that of the conventional one.

Many researchers introduced an experimental works to show the effect of operating temperature, PCMs type and addition of nanoparticles on the on PV system performance. Wei et al. [16] and Hasan et al. [6] showed the effect of highly hot operating temperature on the performance of PV cell. Chandel and Agarwal [5] reported that PCM technologies need to be optimized in terms of its material and the configurations used with the PV panels system. Al Siyabi et al. [2] investigated experimentally the effect of two different PCMs with different thickness and melting temperature for power ratings. Huang et al. [7–11] introduced a different experimental and numerical studies on the integration of a suitable PCM with a PV panel to mitigate the panel temperature rise. The studies verified the likelihood and dominance of the PV–PCM system. The results demonstrated that the temperature rising of the system was reduced by about 30 °C when compared with the datum of a single flat aluminum plate.

Kaviarasu and Prakash [12] demonstrated that despite the high latent heat storage of PCMs, their low thermal property calls for the incorporation of nanomaterials. The results disclosed that the high-surface-to-volume ratio of nanoparticles affected on the thermal properties of the base PCM. Sharma et al. [15] presented a combined cooling solution of a passive type for Building-Integrated Concentrated Photovoltaics (BICPV) by incorporating micro-fins, PCM and nanomaterial-enhanced PCM. The results displayed that there was a reduction in the average temperature at the center of the system of 10.7 °C when micro-fins with PCM was used and 12.5 °C when micro-fins with nanomaterial PCM was used. Al-Waeli et al. [3] experimentally investigated the effect of combined nano-PCM with heat sink configurations with applied heat fluxes on the photovoltaic rear surface temperature. The results displayed that the nano-PCM improved the electrical efficiency of the PV from 8.07 to 13.32%, compared with the conventional PV.

Abdelrahman et al. [1] investigated experimentally the use of PCM to augment the PV performance with fixing hollow copper cylindrical fins at the rear surface of Aluminum plate and submerged this system in tank of RT35HC. The results explored that the enhancement in temperature reduction reached 52.3% by adding the nanoparticles to RT35HC. Accordingly, hollow copper cylindrical fins, PCM and nano-PCM can be successfully used as a TCE to control the PV temperature and increase its efficiency.

Therefore, the present work introduces an experimental study for three different types of PCMs with different operating temperature (RT28HC, RT35HC and RT44HC). Moreover, the used PCMs are used individually pure or mixed with nanoparticles of Al_2O_3, to show their effects on front surface temperature behavior of PV panels. The effect of the following parameters; heat sink configuration, PCM type, PCM- with nanoparticles (Al_2O_3) at various volume fraction and heat flux; 820, 514 and 279 W/m^2 that simulate average solar intensities for June to October, March to May and November to February, respectively, are studied in the present work.

Experimental setup and procedures

The test section presented in Fig. 1 was established and built up by Abdelrahman et al. [1] as a modeling system for PV panel. The test section is constructed from two aluminum surfaces, heating section, Nano-PCM tank and heat sinks. The two aluminum surfaces have dimensions 220 × 110 × 4 mm, those have three grooves to fix the thermocouples to record surfaces temperature. The nano-PCM tank is made from Perspex material and has 10-mm thickness, the depth of tank is 20 mm and its internal dimensions are 220 × 110 mm. Three heat sinks configurations are consisting of hollow cylindrical fins (11, 18 and

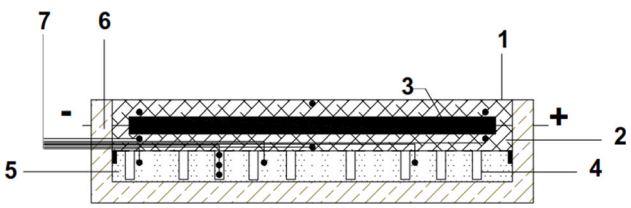

Fig. 1 A schematic drawing for test section [1]

Table 1 Thermophysical properties of RT28HC, RT35HC, RT44HC ([4], Rubitherm data sheet)

Description	RT28HC	RT35HC	RT44HC
Melting range	27–29 °C	34–36 °C	41–44 °C
Main peak	28 °C	35 °C	43 °C
Congealing range	29–27 °C	36–34 °C	44–40 °C
Main peak	27 °C	35 °C	43 °C
Heat storage capacity ± 7.5%	245 kJ/kg	240 kJ/kg	255 kJ/kg
Combination of latent and sensible heat in a range of 21 °C to 36 °C	67 Wh/kg	67 Wh/kg	71 Wh/kg
Specific heat capacity	2 kJ/kg K	2 kJ/kg K	2 kJ/kg K
Density of solid	0.88 kg/l at 15 °C	0.77 kg/l at 25 °C	0.78 kg/l at 25 °C
Density of liquid	0.77 kg/l at 40 °C	0.67 kg/l at 60 °C	0.76 kg/l at 80 °C
Density solid at 15 °C	0.88 kg/l	0.77 kg/l	0.78 kg/l
Density liquid at 40 °C	0.77 kg/l	0.67 kg/l	0.76 kg/l
Heat conductivity (both phases)	0.2 W/m K	0.2 W/m K	0.2 W/m K
Purity	100%	100%	100%
Flash point (PCM)	165 °C	177 °C	186 °C
Max. operation temperature	50 °C	70 °C	70 °C

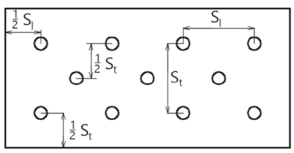

Configuration 1 : 11 fins

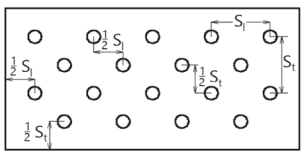

Configuration 2 : 18 fins

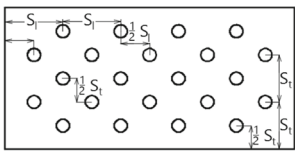

Configuration 3 : 22 fins

Fig. 2 Fins heat sinks configurations

22) made from copper are soldered to a copper sheet which is fixed to the rear aluminum surface. The three configurations have a volume fractions (fins to the PCM container) of 2.85%, 4.67% and 5.7% for fins, 11, 18 and 22, respectively.

Three types of PCMs "RT28HC, RT35HC and RT44HC" are used in the present study. These PCMs are used individually pure or mixed with Al_2O_3 nanoparticles. Table 1 represents the properties of the used PCMs. The nano-PCMs in the current study are prepared by mixing the Al_2O_3 nanoparticles of concentrations from 0.11 to 0.77% by volume, with 0.11% six equal increments, with melted PCM by using ultrasonic vibrator for three hours. The applied voltage to the heating section is regulated by a voltage regulator to simulate the different applied heat fluxes of 279, 514 and 820 W/m^2 in the simulated system.

Figure 2 shows the three staggered configurations configuration of heat sinks at the rear aluminum surface after putting a conductive material to overcome the thermal contact resistance. Each heat sink is constructed of hollow cylindrical copper fins with 20-mm height, 8-mm inner diameter and 2-mm thickness. These fins are soldered to a thin copper plate of 1-mm thickness. The details of heat sinks are presented in Table 2. There are other parameters studied with the three configurations; heat fluxes, pure PCMs and nano-PCMs.

Table 2 Details of the heat sink configurations

Configuration number	S_l, mm	S_t, mm	N	h, mm
1	55	55	11	20
2	44	44	18	20
3	44	36.7	22	20

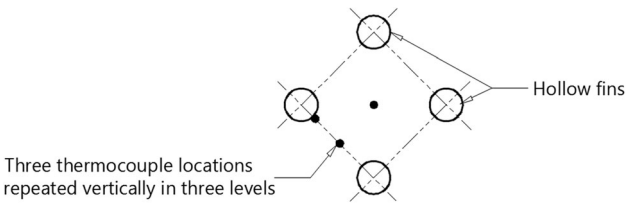

Fig. 3 Thermocouples positions inside PCM tank with heat sink fins

Fig. 4 Three-dimensional of fins soldiered to aluminum plate

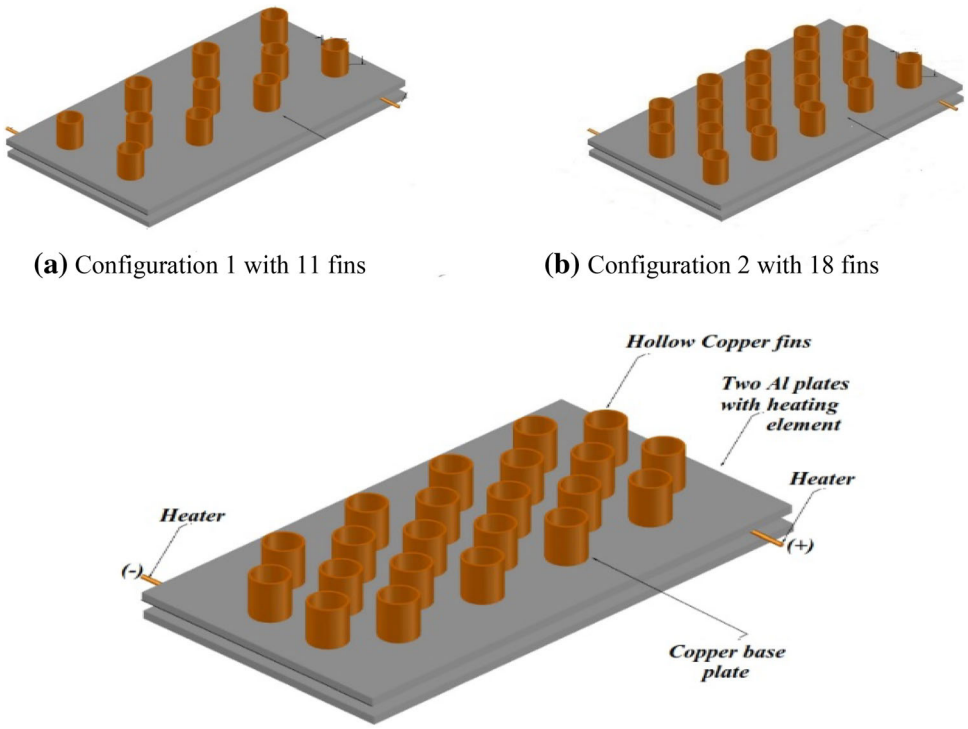

(a) Configuration 1 with 11 fins **(b)** Configuration 2 with 18 fins

(c) Configuration 3 with 22 fins

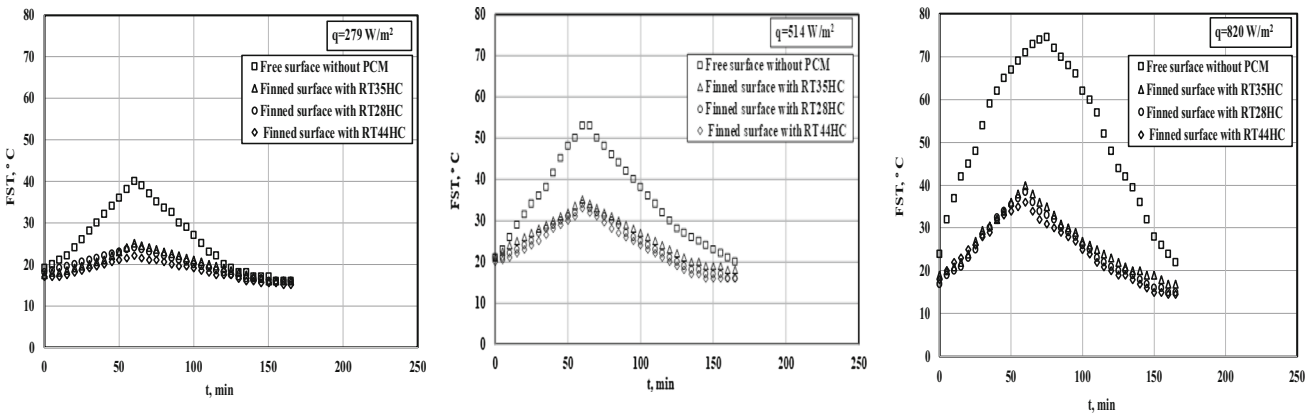

Fig. 5 Front surface temperature variation with time without PCM at T_{∞} = 21 ± 1 °C

As introduced before by Abdelrahman et al. [1], six thermcouples of k-type are distributed on both upper and lower aluminum plates, three on each side, to measure the front and rear surface temperatures. Also, as presented in Fig. 3, three thermocouples are located inside the PCM container with heat sink which repeated vertically in three levels.

Figure 4 shows three dimension of fins configurations and there staggered distributions.

Results and discussion

The experimental setup has been validated with [8] as introduced before by Abdelrahman et al. [1] and a worthy agreement with the former study shows the assurance in the experimental test rig and the measuring techniques. Furthermore, Abdelrahman et al. [1] results revealed that the FST increases as the heat flux increases, and a higher temperature of 74.5 °C was obtained at the highest heat flux of 820 W/m^2 after 75 min. In the current study, several parameters such as heat flux, PCM type, copper fins

configuration and nanoparticles concentrations mixed with PCMs are experimentally investigated. The results of the above-mentioned parameters are presented below to show their effect on the front surface temperature.

Effect of fins configurations

Figure 5 represents the effect of PCM type on FST at $T\infty$ = 21 °C at three heat fluxes of 279, 514 and 820 W/m^2. The figure shows that the temperature increases till reaches the maximum during the charging then it decreases again during the discharging. The same trend is observed for all studied heat fluxes.

Figure 6 shows the variation of front surface temperature with time for exploring the effect of using the three different PCMs and heat sink configurations at different heat flux values and comparing with free surface. It is noted that using heat sinks with PCMs offer advantage for overcoming the drawback of lower PCM thermal conductivity. The figure demonstrates that there are reductions in front surface temperature for all heat sink configurations with three PCM types. The results show that configuration

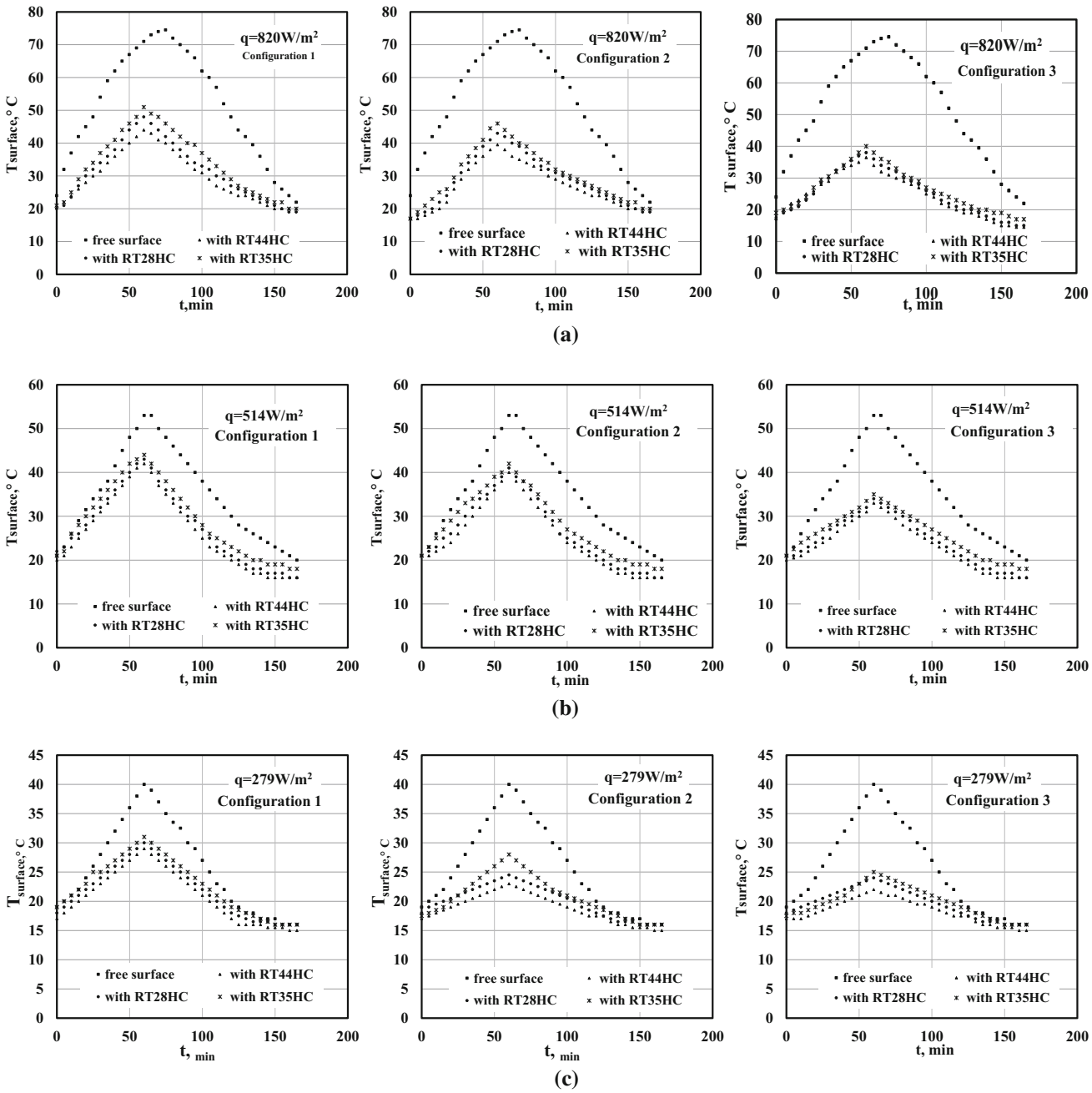

Fig. 6 Effect of configurations on the FST with different PCM **a** Configuration 1 **b** Configuration 2 **c** Configuration 3

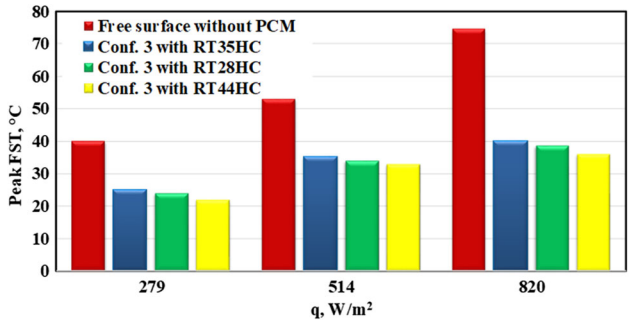

Fig. 7 Effect of PCM type with heat sink configuration 3 on the peak FST at different heat fluxes

3 achieves lower front surface temperature due to having larger numbers of fins when compared with other heat sink configurations. Also, the highest reduction in free surface temperature is obtained for configuration 3 using RT44HC when compared with the base plate at heat flux 820 W/m^2 as a result of its high heat storage capacity.

Effect of PCM type

Figure 7 represents the effect of PCM type on FST for the three heat sinks at T_∞ = 21 °C. It reveals that for a fixed heat flux and configuration, the PCM-type influences the FST. The whole enhancements from the three types of pure PCMs compared to the free surface are represented in Table 3. The results show that RT44HC has the highest enhancement of about 51% compared to the free surface at heat flux 820 W/m^2 with configuration 3. This high enhancement is assigned to the combined effect of configuration and pure PCM (RT44HC) which has high heat storage capacity and combination of latent and sensible heat.

Figure 8 represents the whole enhancement percentage for heat sink configuration 3 with the three types of PCMs compared to the free surface without PCM. The results show that RT44HC has the highest enhancement compared to the other two PCMs at all heat fluxes. Generally, the achieved enhancement is due to the combined effect of finned surface configuration and PCM. Also, the high heat storage capacity and latent and sensible heat combination of RT44HC lead it to have the best performance compared to the other two PCMs.

Effect of mixture (PCM-Nanoparticles)

Figure 9 represents the effect of mixing AL_2O_3 nanoparticles with the three used types of PCMs for the heat sink configuration 3. The effect of PCM type mixed with Al_2O_3 nanoparticles at three different volume fractions of 0.22%,

Table 3 Enhancement percentages of FST compared to the free surface at different heat sink configurations, pure PCM types and heat fluxes

PCM type	Heat flux, W/m^2	Configuration 1 (%)	Configuration 2 (%)	Configuration 3 (%)
RT35HC	820	31.5	38.2	46.3
	514	16.9	24.5	33.9
	279	22.5	30	37.5
RT28HC	820	35.5	42.28	48.9
	514	18.8	26.4	35.8
	279	25	38.75	40
RT44HC	820	40.9	46.9	51
	514	20.7	28.3	37.7
	279	27.5	42.5	45

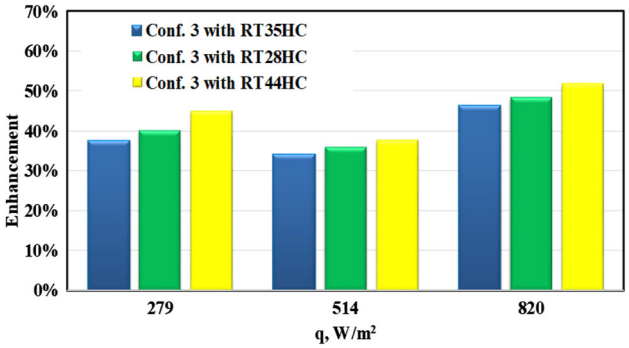

Fig. 8 Enhancement percentages of FST compared to the free surface at different PCM types and heat fluxes = 820 W/m^2

0.44% and 0.77% for configuration no. 3 and heat flux of 820 W/m^2. It demonstrates that adding AL_2O_3 to PCM enhances the FST when compared to the free surface or heat sink configuration with pure PCM. Also, it shows that as the volume concentration of Al_2O_3 nanoparticles increases, it leads to decrease in the temperature of frontal surface. So that, the results indicate that the addition of Al_2O_3 to the PCMs enhance the FST when compared to the free surface or heat sink configuration with pure PCM.

Moreover, the figure demonstrates that for the smallest nanoparticle's concentration through the tested range, 0.11% by volume, there is nearly no effect when compared with the using of pure PCM for all studied PCMs. For configuration 3 and Al_2O_3 nanoparticles concentration of 0.77% at heat flux of 820 W/m^2 are 52.3% and 54.2%, respectively.

Furthermore, the results recorded a highest reduction of 12.5% and 57.7% compared to PCM (RT44HC) only, in the FST at heat flux of 820 W/m^2 when using configuration

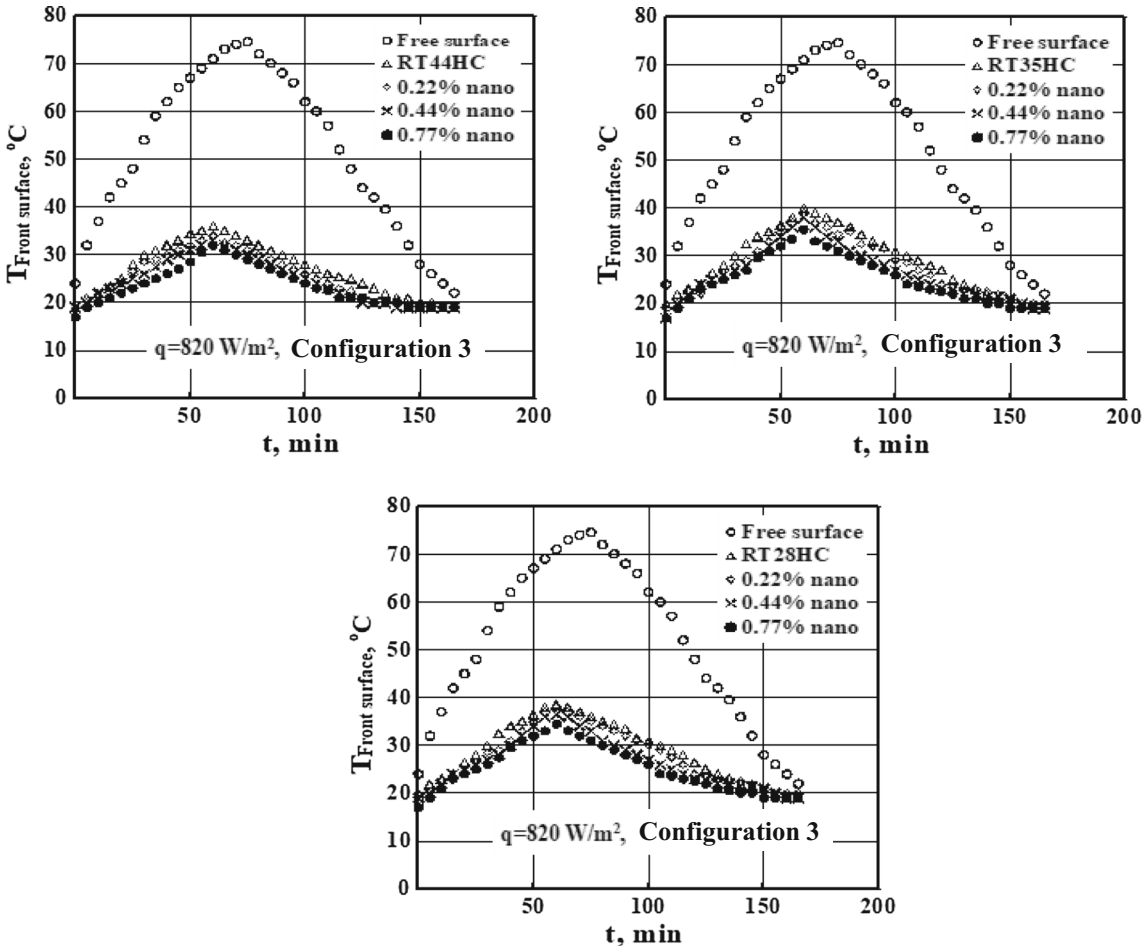

Fig. 9 Effect of PCM-nanoparticles mixture on FST at T_∞ = 21 °C

3 only and with 0.77% nanoparticles concentration, respectively.

Figure 10 shows the enhancement percentage in peak FST compared to the free surface for different pure PCMs and PCM-Al_2O_3 mixtures with concentration of 0.11% to 0.77% with all tested heat fluxes. The figure demonstrates that the high enhancement percentages in peak FST are obtained for the three used types of PCMs and they increased slightly with adding Al_2O_3 to the PCMs. Furthermore, it is noted that the enhancement percentages increase with all nanoparticle's concentration, except for the smallest nanoparticle's concentration of 0.11%, that shows no effect for all studied PCMs when compared with corresponding pure PCM.

The results recorded the highest enhancement in the peak FST of 57% at heat flux of 820 W/m^2 and Al_2O_3 nanoparticles concentration of 0.77% for configuration 3 and RT44HC compared to the free surface. While the pure RT44HC with configuration 3 achieves enhancement in the peak FST of 51.7% when compared to the free surface at the same heat flux.

On the other hand, Fig. 11 shows the enhancement percentage in peak FST for different PCM-Al_2O_3 mixtures with concentration of 0.11% to 0.77% and heat sink configurations at all heat fluxes and compared to the corresponding pure PCM. It is noted that the enhancement percentages increase with an increase in nanoparticle's concentration, except for the smallest nanoparticle's concentration of 0.11%, that shows no effect for all studied PCMs when compared with corresponding pure PCM. The figure demonstrates that the highest enhancement in the peak FST of 11.1% at heat flux of 820 W/m^2 and Al_2O_3 nanoparticles concentration of 0.77% with configuration 3 and RT44HC-Al_2O_3 mixtures when compared with the corresponding pure RT44HC.

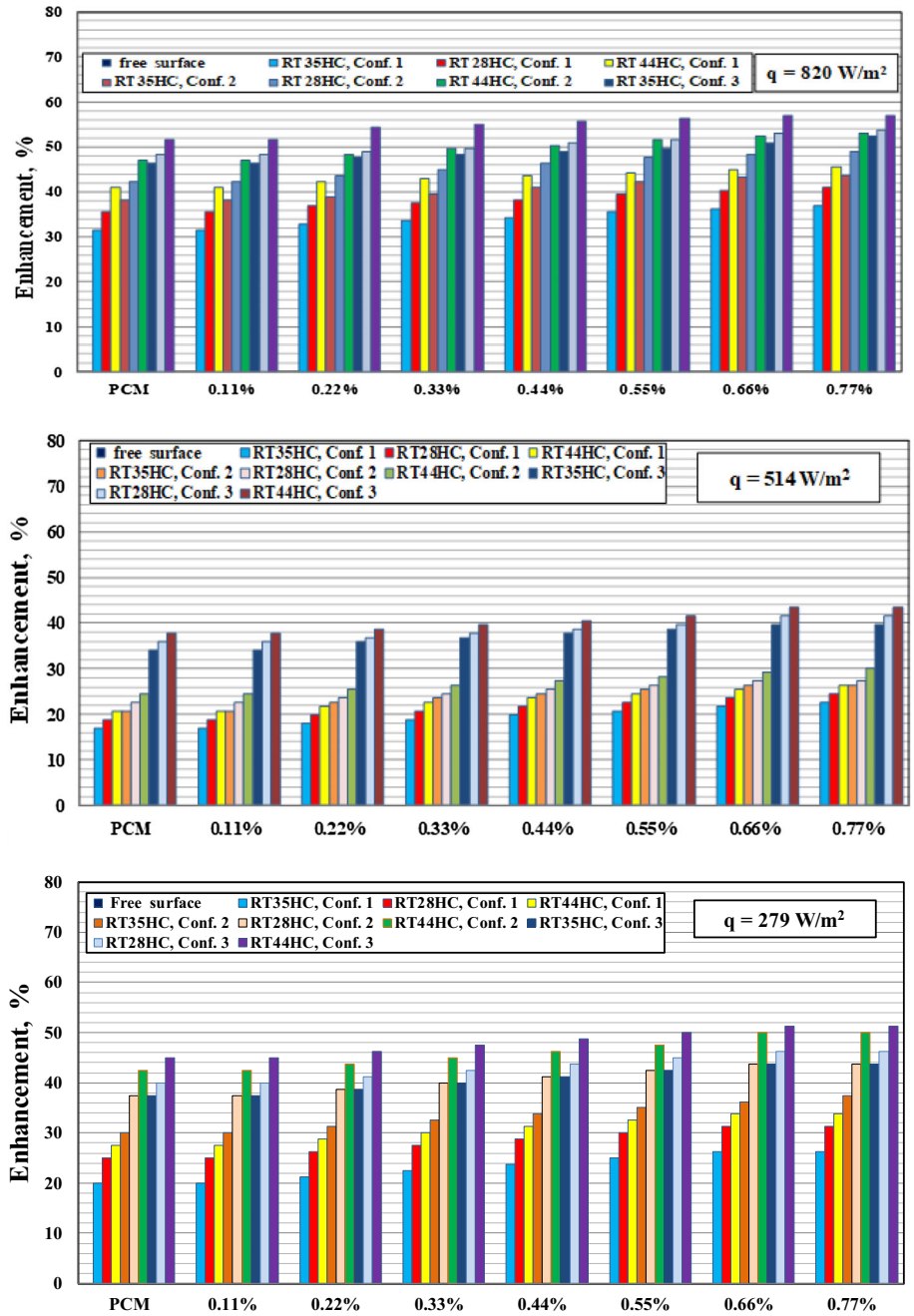

Fig. 10 Enhancement percentage in peak FST of pure PCMs and PCM-nanoparticle mixtures with heat sink configurations (at T_∞ = 21 °C) **a** q = 820 W/m^2, **b** q = 514 W/m^2, **c** q = 279 W/m^2

Conclusions

The present work introduces a study on passive thermal control of photovoltaic cells and comparing different types of PCMs (RT35HC, RT28HC and RT44HC) at different heat fluxes around the year of 820, 514 and 279 W/m^2 to predict and compare the thermal performance of aluminum-heated plate simulating PV solar cell. Experiments are conducted, and the results are obtained for the different mixing types of PCMs with AL_2O_3 nanoparticles at different volume fraction in range of 0.11% to 0.77%, to reach to steady state. The foremost conclusions of the present experimental work are:

- Using PCM reduces the surface temperature of the PV system, and consequently leads to enhancing its performance.
- The results indicate that the enhancement is increased gradually as volume fraction of AL_2O_3 nanoparticles increased in the used Nano-PCMs through the tested range of 0.11% to 0.77%.

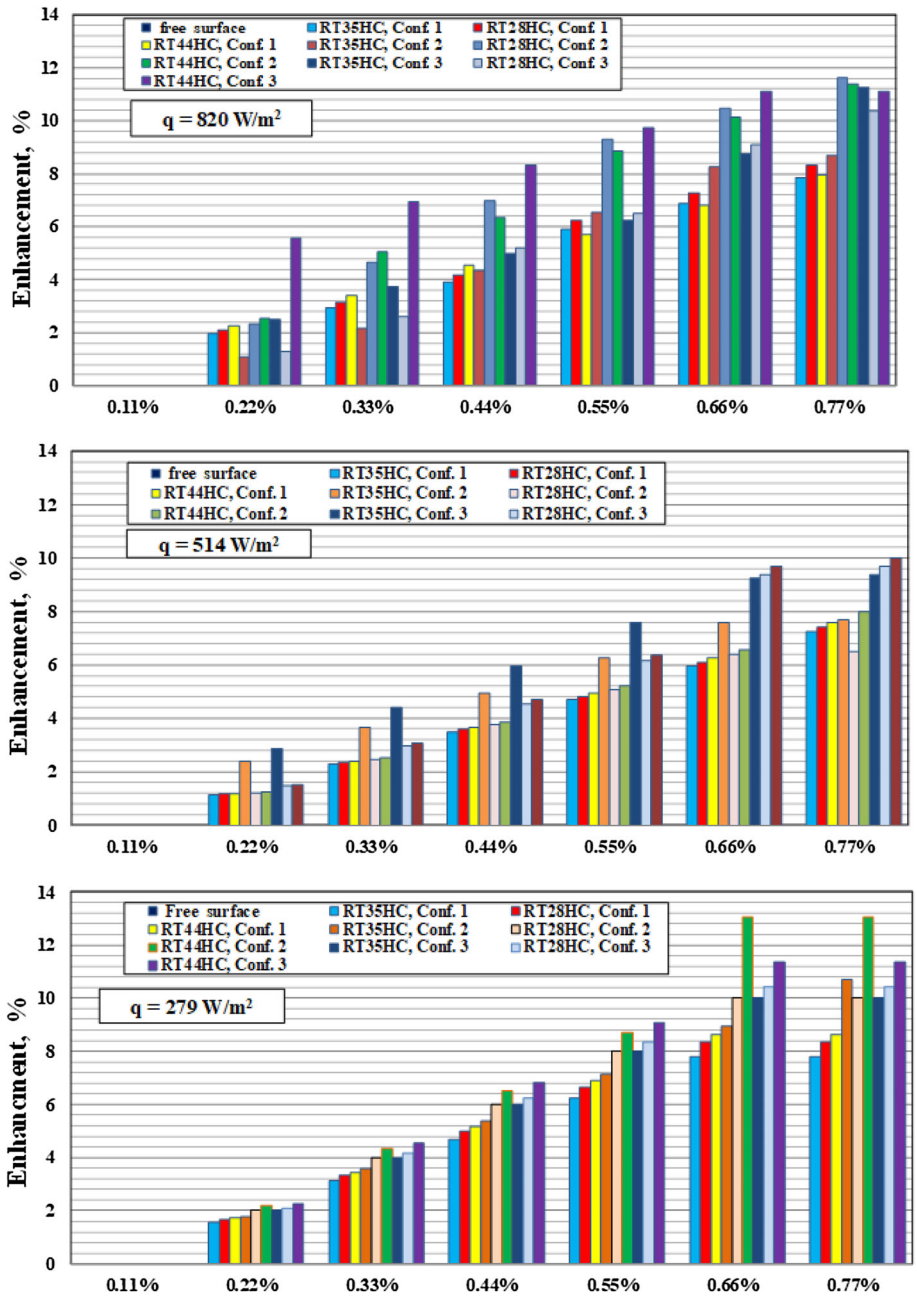

Fig. 11 Enhancement percentage in peak FST of PCM-nanoparticle mixtures with heat sink configurations (at T_∞ = 21 °C) **a** q = 820 W/m^2, **b** q = 514 W/m^2, **c** q = 279 W/m^2

- The highest reductions in the FST are 52.3%, 54.2% and 57.7% which occurred with configuration 3, heat flux of 820 W/m^2 and AL_2O_3 nanoparticles concentration of 0.77% for PCMs types RT35HC, RT28HC, and RT44HC, respectively.
- Using nanoparticles with PCM reduce the FST of the simulated PV cells which means that the life time of photovoltaic cell will be increased.

References

1. H.E. Abdelrahman, M.H. Wahba, H.A. Refaey, M. Moawad, N.S. Berbish, Performance enhancement of photovoltaic cells by changing configuration and using PCM (RT35HC) with nanoparticles Al_2O_3. Sol. Energy **177**, 665–671 (2019). **ISSN 038-092X.**
2. I. Al Siyabi, S. Khanna, T. Mallick, S. Sundaram, Multiple phase change material (PCM) configuration for PCM-based heat sinks. An Experimental Study. Energies **11**(7), 1629 (2018)
3. A.H.A. Al-Waeli, K. Sopian, H.A. Kazem, J.H. Yousif, M.T. Chaichan, A. Ibrahim, S. Mat, H. Ruslan, Mohd, Comparison of prediction methods of PV/T nanofluid and nano-PCM system

using a measured dataset and artificial neural network. Sol. Energy **162**, 378–396 (2018). **ISSN 038-092X**
4. Anon, *Rubitherm Data Sheet of RT35HC* (Rubitherm GmbH, Hamburg, 2013)
5. S.S. Chandel, T. Agarwal, Review of cooling techniques using phase change materials for enhancing efficiency of photovoltaic power systems. Renew. Sustain. Energy Rev. **73**, 1342–1351 (2017)
6. H.A. Hasan, K. Sopian, A.H. Jaaz, Ali N. Al-Shamani, Experimental investigation of jet array nanofluids impingement in photovoltaic/thermal collector. Solar Energy **144**, 321–334 (2017). **ISSN 038-092X**
7. M.J. Huang, P.C. Eames, B. Norton, Thermal regulation of building-integrated photovoltaics using phase change materials. Int. J. Heat Mass Transf. **47**(12–13), 2715–2733 (2004)
8. M.J. Huang, P.C. Eames, B. Norton, Phase change materials for limiting temperature rise in building integrated photovoltaics. Sol. Energy **80**(9), 1121–1130 (2006)
9. M.J. Huang, The effect of using two PCMs on the thermal regulation performance of BIPV systems. Sol. Energy Mater. Sol. Cells **95**, 957–963 (2011)
10. M.J. Huang, *Two phase change material with different closed shape fins in building integrated photovoltaic system temperature regulation* (World Renewable Energy Congress, Sweden, 2011)
11. M.J. Huang, P.C. Eames, B. Norton, N.J. Hewitt, Natural convection in an internally finned phase change material heat sink for the thermal management of photovoltaics. Solar Energy Mater Sol Cells **95**(7), 1598–1603 (2011)
12. C. Kaviarasu, D. Prakash, Review on phase change materials with nanoparticle in engineering applications. J. Eng. Sci. Technol. Rev. **9**(4), 26–386 (2016)
13. S. K. Saha, K. Srinivasan, P. Dutta, Studies on optimum distribution of fins in heat sinks filled with phase change material, J/ Heat Transfer, 2008;130
14. S.K. Saha, P. Dutta, Thermal management of electronics using pcm-based heat sink subjected to cyclic heat load. IEEE Trans. Compon. Packag. Manuf. Technol. **2**, 464–473 (2012)
15. S. Sharma, L. Micheli, W. Chang, A.A. Tahir, K.S. Reddy, T.K. Mallick, Nano- enhanced phase change material for thermal management of BICPV. Appl. Energy **208**, 719–733 (2017)
16. N. T. J. Wei, W. J. Nan, C. Guiping, Experimental study of efficiency of solar panel by phase change material cooling. International Conference on Materials Technology and Energy IOP Conf. Series: Materials Science and Engineering 217 2017